Journal of the Taiwan Institute of Chemical Engineers 93 (2018) 554–565

Contents lists available at ScienceDirect

Journal of the Taiwan Institute of Chemical Engineers

journal homepage: www.elsevier.com/locate/jtice

Process design and potential use of a regenerable biomagsorbent for effective decolorization process

Rukiye Karagöz[a], Sibel Tunali Akar[b], Serpil Turkyilmaz[c], Sema Celik[b], Tamer Akar[b,*]

[a] Department of Chemistry, Graduate School of Natural and Applied Sciences, Eskişehir Osmangazi University, 26480 Eskişehir, Turkey
[b] Department of Chemistry, Faculty of Arts and Science, Eskişehir Osmangazi University, 26480 Eskişehir, Turkey
[c] Department of Statistics, Faculty of Arts and Science, Bilecik Şeyh Edebali University, 11210 Bilecik, Turkey

ARTICLE INFO

Article history:
Received 24 April 2018
Revised 29 August 2018
Accepted 1 September 2018
Available online 2 October 2018

Keywords:
Biosorption
Decolorization
Modification
Process design
Regeneration

ABSTRACT

Aquatic pollution caused by synthetic dyes poses a significant threat to environment and public health. Efficient and convenient removal of dye contaminants from aquatic environment is a challenge for environmental protection. Biosorption process is a promising way to remove such chemicals from contaminated media. Herein, a new biomagsorbent based on *Lactarius salmonicolor* cells (MagLS) was simply designed by combining magnetic separation and biosorption techniques. Technical feasibility of the prepared biomagsorbent for Reactive Yellow 2 retention was examined. The interactive effects of batch process variables were evaluated by 4 – level Box–Behnken design. Kinetic analysis indicated applicability of the pseudo – second – order model. q_{max} value was noted as 115.23 mg/g and retention of RY2 was endothermic and spontaneous in nature. IR, SEM/EDX analysis and zeta potential measurements were employed for the characterization. Flowthrough experiments indicated that MagLS has a high decolorization potential. Regeneration experiments carried out in 25 consecutive cycles revealed that MagLS can be easily regenerated and reused for at least 15 cycles with high sorption (~70%) and desorption (~80%) yield. Furthermore, after 25 cycling process, a recovery yield of RY2 dye was maintained at around 80%.

1. Introduction

The intensive industrial activities throughout the world have led to increasing generation of industrial wastewaters. This type of wastewaters contain different organic and inorganic contaminants. Sythetic dyes are used in several industrial branches including textile, paint, leather, plastic, paper etc. and represent the hazardous water contaminant as important class of organic pollutants. Direct discharge of the colored effluents from industrial sources causes biological and chemical changes and visual pollution in the aquatic ecosystem. Additionally, synthetic dyes can create toxicity symptoms on living tissues depending on length of exposure and their concentrations. Therefore, in recent years there is a growing interest to reduce environmental impact of colored effluents [1,2]. Biosorption is a promising alternative treatment method for the removal of various types of pollutants from contaminated waters. This method has potential advantages such as low operation cost, versatility, simplicity, high degree and rate of uptake, pollutant recovery, analogous operation to traditional ion exchange method and easy availability of biomass and waste biomaterials [3,4]. The most of the biosorption studies are carried out with the biomasses obtained from fungi, bacteria, microalgae, agricultural waste, industrial waste, plant residues, cellulose and chitosan derived materials etc. Depending on the biomaterial type, functional groups such as carbonyl, carboxyl, amide, amine, imine, hydroxyl, imidazole, sulfhydryl, sulfonate, thiol, phosphate, and phosphodiester present on the biomaterial surface are responsible for sequestering pollutants [5]. Nevertheless, the drawback of the biosorption applications is the difficulty to separate the powder form of biomaterial particles from the treated aquatic media. In this context, magnetically modified sorbent materials have been received growing attention because they can be easily separated from aquatic media by using a simple external magnetic field after the sorption process. Less energy consumption, shorter separation time and better selectivity are other important advantages of magnetic separation process [6,7]. It is also useful in both small and large scale applications [8].

Different types of magnetically modified sorbent materials have been effectively used for the separation of various pollutants from aquatic media [9–16]. However, so far only limited knowledge exists concerning the adaptation of magnetic separation process to microbial cells for the treatment of dye contaminated waters. Magnetically modified *Saccharomyces cerevisiae* [8], *Kluyveromyces*

* Corresponding author.
E-mail address: takar@ogu.edu.tr (T. Akar).

https://doi.org/10.1016/j.jtice.2018.09.001
1876-1070/

fragilis [17], *Chorella vulgaris* [18] and *Penicillium janthinellum* [19] cells are a few examples of this type of biosorbents.

Therefore, in this work, an application of magnetically modified *Lactarius salmonicolor* (MagLS) was considered as a biomagsorbent for removing Reactive Yellow 2 (RY2) from aquatic media via sorption process. To our knowledge, there is no literature report concerning the preparation and use of MagLS for any purpose. Response surface methodology (RSM) combined with Box-Behnken design (CCD) was used to examine the interactive effects of important operational parameters and to recognize the efficiency of the experimental system. The batch biosorption characteristics for the natural biomass and MagLS were examined. The isotherm and kinetic models and thermodynamic parameters were employed to identify the decolorization behavior of the suggested sorbent. Zeta potential measurements, SEM, EDX, XRD and IR analysis were employed to identify the sorbent characteristics. Desorption and regeneration properties of the developed sorbent material were also investigated in addition to breakthrough curve analysis.

2. Materials and method

2.1. Chemicals

The target pollutant in this study (RY2 dye) is obtained from Sigma–Aldrich. All other reagents and chemicals used in this work are of analytical grade.

2.2. Preparation of MagLS

The fresh samples of mushroom were collected from Gemlik, Turkey. The fruit bodies of *L. salmonicolor* were rinsed with deionized water and later dried in an oven at 60 °C for overnight. Dried mushroom biomass was ground using IKA A – 11 laboratory mill and sieved to select the particle size less than 212 µm. A stock RY2 solution was prepared at a concentration of 1.0 g/L. Different concentrations of dye were freshly prepared from this stock solution. pH values of the test solutions were adjusted with 0.1 mol/L HCl or NaOH solutions. Co-precipitation method was used for the preparation of MagLS [20]. $FeSO_4 \cdot 7H_2O$ (2.1 g) and $FeCl_3 \cdot 6H_2O$ (3.1 g) were dissolved in distilled water (80 mL). While this mixture was heated to 80 °C, 10 mL of NH_4OH solution (25%) was added. Then, 10 g of the powdered *L. salmonicolor* was suspended in this mixture under vigorously stirring for 30 min at 80 °C. The suspension was then cooled to room temperature. Finally, the magnetite coated *L. salmonicolor* was completely separated by a magnet, repeatedly washed with double distilled water, dried and then ground to obtain powdered form of MagLS. Magnetic particles are stable in the sorbent structure. The interactions between the magnetic particles and the biomass are strong enough to provide sorbent stability.

Fig. 1 shows chemical structure of RY2, powdered form of MagLS and RY2 solutions before and after magnetic separation process.

2.3. Instrumentation

Infrared (IR) spectra of biomagsorbent before and after decolorization were generated by using IR spectrophotometer (Bruker Tensor, 27) in the wavenumber range of 400–4000 cm^{-1} using KBr pellet technique. The surface morphologies were examined by a scanning electron microscope (SEM, JEOL 560 LV) equipped with energy dispersive X – ray (EDX) analysis. The acceleration voltage and image magnification were used as 20 kV and × 1500, respectively. EDX analysis was also conducted during SEM imaging. In order to improve image quality and electron conductivity, samples were coated with thin layer of palladium and gold in a Polaron SC – 7620 Sputter Coater. The powder XRD analysis was performed by a polycrystalline X-ray diffractometer (Empyrean PANalytical). Zeta potential measurements over the pH range of 1.0 – 5.0 were performed using a zeta sizer (Malvern Zeta sizer nano ZS). Vibrating Sample Magnetometer (VSM) (Lakeshore VSM 7407) was employed to analyze the magnetic properties of the sorbent at room temperature. The pH measurements were conducted by a pH meter (WTW – Inolab 720). Dye concentrations in the solutions were determined using Shimadzu UV – 2550 UV–vis spectrophotometer.

2.4. Batch and continuous mode decolorization experiments

Batch decolorization experiments were carried out in 100 mL flasks at 120 rpm agitation speed in order to identify the effects of operational parameters including pH, contact time, biosorbent amount and initial RY2 concentration. The sorption mixtures were placed in a temperature controlled orbital shaker at 20 °C and shaken at a speed of 120 rpm. At the end of the batch mode experiments, MagLS was easily and completely separated from the solution by a magnet. On the other hand LS was separated from the sorption mixture by centrifugation at 4500 rpm for 5 min. The supernatans were collected to determine the final dye concentration by a UV spectrophotometer at a maximum wavelength of 404 nm.

Glass columns with an internal diameter of 11 mm were used in the continuous mode decolorization studies. The columns were packed with a known amount of LS and MagLS to yield the desired bed height. The biosorbent was supported between a layer of glass wool at the top and the bottom of the columns. The experiments were carried out by pumping dye solutions (25 mL, 100 mg/L) through the column in down-flow mode using a peristaltic pump (Ismatec IP16). Column decolorization performances of the suggested sorbents were studied at different flow rates (0.5, 1.0, 2.0, 3.0 and 6.0 mL/min) and sorbent amounts (0.01, 0.015 0.02, 0.03, 0.04, 0.06, 0.08, 0.10 and 0.15 g) at an inlet pH of 2.0. Tygon tubings were used for the connection between columns and peristaltic pump. The dye concentration in the effluent was analyzed as mentioned above.

Decolorization yield and the equilibrium amount of RY2 sorbed onto per unit mass of biomagsorbent were calculated by the following expressions:

$$\text{Decolorization yield}(\%) = \frac{(C_i - C_e)}{C_i} \times 100 \quad (1)$$

$$q_e = \frac{V(C_i - C_e)}{m} \quad (2)$$

where C_i and C_e (mg/L) are the initial and the equilibrium RY2 concentrations in the aqueous phase, V (L) is the volume of RY2 solution, m (g) is the weight of sorbent material and qe (mg/g) is the sorption capacity.

2.5. Design of the decolorization process

In the present work a subset of Response Surface Methodology (RSM) known as Box-Behnken design was employed to evaluate the effects of selected variables. According to employed model the number of the required experimental run was calculated from the following equation:

$$N = 2k \times (k - 1) + \text{cp} \quad (3)$$

where N, k and cp represent the number of experimental runs, the factor number and the replicate number of the central point, respectively [21–23]. The decolorization yield was chosen as the dependent output response variable. Four independent variables of initial pH (x_1), sorbent amount (x_2), contact time (x_3) and dye concentration (x_4) were coded at three levels between 1 and + 1, and these variables were manipulated in the range of pH 2–8

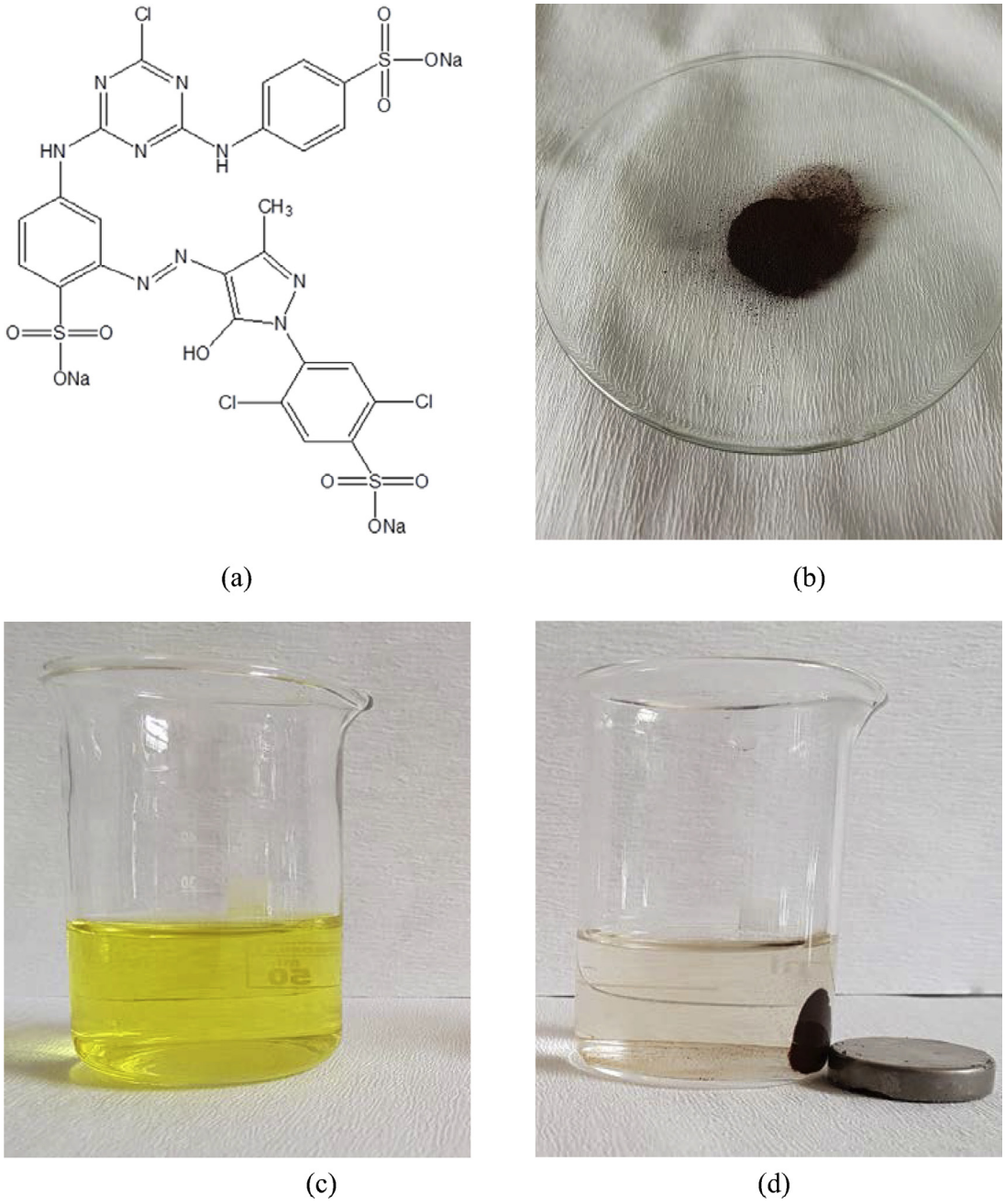

Fig. 1. Chemical structure of RY2 dye (a), powdered form of MagLS (b) and RY2 solutions before (c) and after (d) magnetic separation.

for initial pH, 0.025 – 0.2 g/L for biomass amount, 5 – 90 min for contact time and 50–750 mg/L for initial dye concentrations.

The factor variables are coded according to following transformation:

$$X_i = (x_i - x_0)/\Delta x_i \quad (4)$$

where X_i and x_i are coded and the real value of independent variable, respectively. x_0 is the real value of independent variable of the centre point, and Δx_i is the step change of the real value.

The statistical model which indicates relationships independent variables (factors) and response variable (Y) has been obtained by using multiple linear regression model. For this purpose; linear, quadratic and interaction effect terms of variables have been displayed in the regression model as Eq. (5)

$$Y = \beta_0 + \sum_{i=1}^{m} \beta_i X_i + \sum_{i=1}^{m} \beta_{ii} X_i^2 + \sum_{i=1}^{m-1} \sum_{j=i+1}^{m} \beta_{ij} X_{ij}, m = 1, 2, 3, 4. \quad (5)$$

A system with four independent variables (factors) (X_1, X_2, X_3, X_4) and the response variable (Y) can be represented by a multiple linear regression model;

$$Y = \beta_0 + \beta_1 X_1 + \beta_2 X_2 + \beta_3 X_3 + \beta_4 X_4 + \beta_{12} X_1 X_2 + \beta_{13} X_1 X_3 + \beta_{14} X_1 X_4 + \beta_{23} X_2 X_3 + \beta_{24} X_2 X_4 + \beta_{34} X_3 X_4 + \beta_{11} X_1^2 + \beta_{22} X_2^2 + \beta_{33} X_3^2 + \beta_{44} X_4^2$$

Where, Y is the response variable (sorption yield of RY2). X_1, X_2, X_3 and X_4 are the levels of factor variables (pH, biosorbent amount, contact time and dye concentration. β_0 is the regression coefficient at the center point; β_1, β_2, β_3 and β_4 are linear effect

coefficients; and β_{12}, β_{13}, β_{14}, β_{23}, β_{24} and β_{34} are interaction effect coefficients. In addition, β_{11}, β_{22}, β_{33} and β_{44} are quadratic effect coefficients. The fitting of the regression model was determined by the coefficient of determination (R^2). Design–Expert Software version 8.0. was used to statistical, regression and graphical analysis of the data. F–test was used to interpret the coefficients.

2.6. Kinetic and isotherm modeling

In order to evaluate the decolorization and the equlibrium time, sorption kinetics was investigated. Kinetic experiments were conducted using an initial RY2 concentration of 200 mg/L and at different temperatures (20, 30 and 40 °C) at predetermined optimum conditions. Kinetic data were analyzed using pseudo – first – order model of Lagergren (Eq. 6) [24], pseudo – second – order model (Eq. 7) [25] and intraparticle diffusion model (Eq. 8) [26].

$$\ln(q_e - q_t) = \ln q_e - k_1 t \quad (6)$$

$$\frac{t}{q_t} = \frac{1}{k_2 q_e^2} + \frac{1}{q_e} t \quad (7)$$

$$q_t = k_p t^{1/2} + C \quad (8)$$

where k_1 (min^{-1}), k_2 (g/mg/min) and k_p ($mg/g/min^{1/2}$) are the pseudo – first – order, the pseudo – second order and intraparticle diffusion rate constants, respectively. q_t (mg/g) is amount of dye adsorbed at time t, respectively. C is the constant related to the thickness of the boundary layer.

Equilibrium experiments were conducted with different initial dye concentrations (50–750 mg/L) at 20, 30 and 40 °C under the optimized conditions. The Langmuir (Eq. 9) [27], Freundlich (Eq. 10) [28] and Dubinin – Radushkevich (D – R) (Eqs. 11–12) [29] isotherm models were employed to analyze the equilibrium data.

$$q_e = \frac{q_{max} K_L Ce}{1 + q_{max} K_L} \quad (9)$$

$$q_e = K_F C_e^{1/n} \quad (10)$$

$$\ln q_e = \ln q_m - \beta \varepsilon^2 \quad (11)$$

$$\varepsilon = RT \ln(1 + 1/C_e) \quad (12)$$

where q_{max} and q_m are sorption capacity of the sorbent material (mol/g), C_e is the dye concentration in solution at equilibrium (mol/L) and K_L is Langmuir equilibrium constant (L/g), K_F (L/mg) is the Freundlich constant and n is the heterogeneity factor. β is the activity coefficient related to the biosorption energy, ε is the Polanyi potential, R (J/mol/K) is the gas constant and T (K) is the absolute temperature.

The separation factor (R_L) can be calculated by Eq. (13) using Langmuir model and indicates the biosorption reaction favorable or unfavorable.

$$R_L = \frac{1}{1 + K_L C_o} \quad (13)$$

If the value of separation factor lies between 0 and 1 it shows a favorable sorption, while separation factor > 1 represents unfavorable adsorption; separation factor = 1 indicates a linear sorption, and separation factor = 0 determines an irreversible adsorption [30].

A mean biosorption free energy (E) may be calculated by Eq. (14) using D – R isotherm. If its value is less than 8 kJ/mol, sorption is in physical form, and if it lies between 8 and 16 kJ/mol, chemical sorption is dominant [31].

$$E = 1/(2\beta)^{1/2} \quad (14)$$

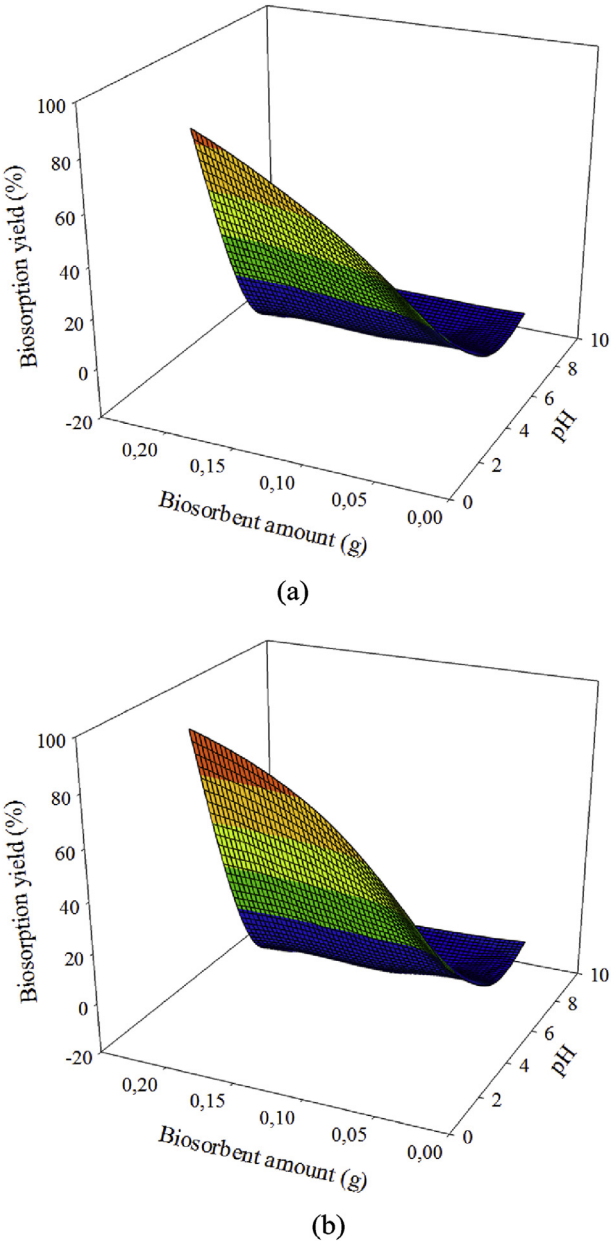

Fig. 2. 3D response surface graphs for the interactive effects of pH and sorbent amount on decolorization yield of LS (a) and MagLS (b).

3. Results and discussion

3.1. Process design and statistical analysis

Decolorization experiments were planned according to the Box – Behnken design to obtain a multiple regression model consisting of 29 trials plus 3 – center points. The coded and actual values of factor variables as well as observed and predicted decolorization yields for MagLS and LS are presented in Supplementary Material (SM1) and (SM2), respectively. Eqs. (15 and 16) indicate the relationship between the predicted responses and independent variables for these sorbent materials obtained from multiple regression analysis.

$$\begin{aligned} y(\text{MagLS}) = {} & 1.83 - 35.25x_1 + 5.60x_2 + 3.43x_3 - 1.98x_4 - 18.16x_1x_2 \\ & - 10.62x_1x_3 + 8.43x_1x_4 - 0.28x_2x_3 \\ & + 0.15x_2x_4 - 0.035x_3x_4 + 34.95{x_1}^2 - 1.85{x_2}^2 \\ & + 0.78{x_3}^2 + 0.66{x_4}^2 \end{aligned} \quad (15)$$

$$y(LS) = -29.66x_1+5.19x_2+2.50x_3-0.42x_4-15.42x_1x_2-7.49x_1x_3 +1.82x_1x_4+0.16x_2x_4+29.56{x_1}^2 -0.76{x_2}^2+2.41{x_3}^2-1.37{x_4}^2 \quad (16)$$

The adequacies of these quadratic models were assessed using analysis of variance (ANOVA) and the corresponding results are presented in SM3 and SM4. Higher values of determination coefficients ($R^2 = 0.942$ for MagLS and $R^2 = 0.947$ for LS) between the predicted and experimental decolorization yield (%) were recorded. *F* values were determined as 16.39 and 17.76 for MagLS and LS, respectively. Moreover the Prob-*F* values for both sorbent were less than 0.0001. These findings imply that the applied quadratic models could be reliable for predicting the decolorization yield. Similarly, it was found that $p-$values for x_1, x_1x_2 and ${x_1}^2$ were less than 0.05, indicating that these variables were statistically significant for decolorization of RY2 by LS and MagLS.

3.2. Effects of significant model components on decolorization efficiency

According to ANOVA results in SM3 and SM4, the effects of pH and sorbent amount were found to be more significant than the other parameters investigated. Therefore, the interactive effects of solution pH and sorbent dosage on RY2 removal by MagLS and LS were given as three dimentional (3D) surface plots in Fig. 2. It was observed that the decolorization yields of MagLS and LS increased with decreasing pH and increasing sorbent amount. The major effects of pH and sorbent amount parameters on the removal process are further verified by the recorded *F* values.

The higher decolorization efficiency (%) at lower pH values (pH 2.0) could be due to the attractive forces between protonated sorbent functional groups and anionic dye molecules. In other words, the functional groups present on the surface of the sorbent material are protonated and acquire a net positive charge at highly acidic conditions. This causes a high electrostatic attraction between the sorbent surface and RY2 molecules, resulting in a high sorption capacity. When the pH of the solution increased, the number of negatively charged sites increased as a result of the deprotonation of sorbent functional groups. Lower sorption capacities of RY2 observed at higher pH values can be attributed to competition between the negatively charged RY2 molecules and the excess hydroxyl ions for the sorption sites. This finding was confirmed by the zeta potential values of these sorbents in Fig 3. The point of zero charges (pzc) of MagLS and LS were determined as 2.25 and 2.15, respectively. At pH less than isoelectric point, the surface charge of adsorbent is positive due to the presence of the high concentration of protons in the environment. Therefore, the positively charged sorbent materials can effectively remove negatively charged dye molecules [32].

On the other hand, increasing decolorization efficiency by increasing sorbent amount can be explained by the increased surface area and the availability of more binding sites. The optimum sorbent dosages are recorded as 1.488 and 2.012 g/L for MagLS and LS, respectively. A higher decolorization yield obtained with a small amount of MagLS when compared with LS is another advantage of MagLS in addition to easy of separation. With the introduction of magnetic particles, the biomass gained magnetic properties and its sorption capacity was simultaneously improved. The similar antagonistic effects of pH and sorbent amount were reported for the sorption of Reactive Blue 19 onto multi – walled carbon nano tubes [33] and *L* – arginine – functionalized Fe_3O_4 nanoparticles [32].

3.3. Decolorization kinetics

Fig. 4 depicts the sorption of RY2 sorbed on LS and MagLS at different temperatures and various time ranges. It is apparent that dye molecules were rapidly sorbed on the biomass preparations in the first 40 min. Thereafter, the decolorization was slower and finally attained equilibrium within 60 min. Fig. 4 also displays the fact that the uptake of RY2 by LS did not significantly changed with temperature ($p > 0.05$). Rapid initial decolorization can be explained by the contacts of dye molecules with available surface sorption sites while subsequent gradual sorption may be attributed to uptake of dye molecules into the sorbent pores [34]. The rapid decolorization kinetics has been evaluated as an important advantage in the practical applications. Because this feature provides high efficiency and economy with the smaller reactor volumes [35]. On the other hand, RY2 sorption capacity of MagLS slowly increased with temperature rising. It was even more pronounced when the temperature rised to 20 °C from 30 °C. This increase was due to the easier diffusion of dye molecules onto the surface of MagLS at higher temperature.

The pseudo – first – order, the pseudo – second – order and intraparticle diffusion models were employed to simulate the kinetics of RY2 decolorization process by the sorbent preparations. The parameters of these kinetic models as well as the coefficients of determination are presented in Table 1. The experimental q_e (exp) values were not in a good agreement with the calculated q_e (cal) values. Also, coefficients of determination values were found as quite low for the pseudo – first – order model. These findings indicated that the pseudo – first – order model was not suitable for modeling the decolorization. On the contrary, the coefficients of determination for the pseudo – second – order model were quite high (0.999) at all the studied temperatures. Furthermore, there is a good agrrement between the values of q_e (cal) and q_e (exp) predicted by this model. These findings indicated that the pseudo – second – order model is favorable kinetic model for the sorption of RY2 onto LS and MagLS at various temperatures. Increasing trend of the rate constant values with an increase in the temperature indicated that the decolorization process is rate – controlled.

The intra – particle diffusion model was also used by plotting uptake versus the square root of time (figure not shown) to identify the decolorization. Although r^2 values obtained for this model are lower than those of the pseudo – second – order model (Table 1), good linearization of the data were observed up to equilibrium for both sorbent. This finding indicates that the decolorization process may be followed by this model up to equilibrium. Since the linear portion of the fitting curve obtained do not pass through the origin, the intraparticle diffusion was not the only rate – limiting step and probably other kinetic models may be controlling the rate of decolorization.

3.4. Isotherm models

The equilibrium data obtained from the sorption process are generally represented by sorption isotherms. The isotherm models provide important parameters for the efficiency and applicability of sorbent material and prediction of the pollutant removal mechanism. In the present study equilibrium data were analyzed by employing Freundlich, Langmuir and Dubinin–Radushkevich (D–R) isotherms. The general isotherm plots for the biosorption of RY2 onto MagLS and LS are included in Fig. 5. The sorption capacities increased with increasing dye concentration and progressively reached a saturation point. The obtained parameters from these models are presented in Table 2. As shown in this table, Langmuir isotherm is more suitable model for the description of equilibrium data with coeeficient of determination (R^2) values greater than 0.985. This finding emphasizes the formation of monolayer coverage with RY2 molecules at specific homogeneous sites on LS and MagLS surfaces. The maximum monolayer sorption capacities were recorded as 1.11×10^{-4} mol/g (96.90 mg/g) and $1.32.10^{-4}$ mol/g

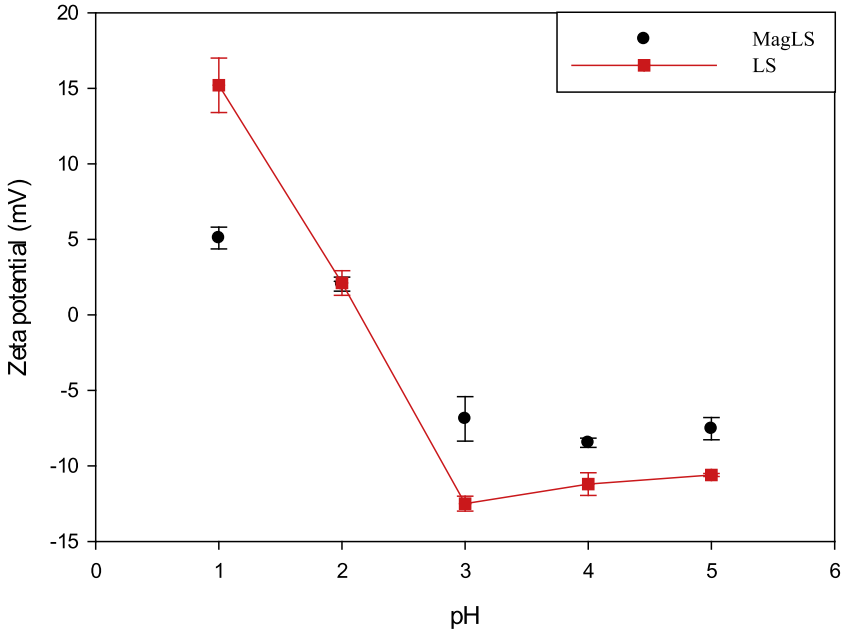

Fig. 3. Zeta potentials of LS and MagLS at various pH values.

Table 1
Kinetic parameters for the biosorption of RY2 onto MagLS and LS.

	Pseudo – first – order				Pseudo – second – order			Intraparticle diffusion		
	t (°C)	k_1 (min^{-1})	q_e (mg/g)	R^2	k_2 (g mg/min)	q_e (mg/g)	R^2	k_p (mg/g /min)	C (mg/g)	R^2
MagLS	20	5.26×10^{-2}	56.43	0.923	7.60×10^{-4}	104.71	0.999	7.92	27.32	0.973
	30	5.41×10^{-2}	48.91	0.911	9.16×10^{-4}	110.77	0.999	7.29	40.25	0.972
	40	4.75×10^{-2}	28.79	0.789	1.23×10^{-3}	111.14	0.999	7.52	45.95	0.941
LS	20	4.40×10^{-2}	27.94	0.914	1.83×10^{-3}	82.10	0.999	4.55	40.12	0.978
	30	4.31×10^{-2}	19.49	0.891	2.04×10^{-3}	80.71	0.999	3.88	43.79	0.930
	40	3.88×10^{-2}	16.44	0.844	2.96×10^{-3}	79.43	0.999	3.44	48.95	0.941

Table 2
Isotherm parameters for the biosorption of RY2 onto MagLS and LS.

	Freundlich					Langmuir			Dubinin – Radushkevich (D – R)			
	t (°C)	n	K_F(L/g)	R^2	q_{max} (mol/g)	K_L (L/mol)	R_L	R^2	q_m (mol/ g)	β (mol^2 /kJ^2)	R^2	E (kj mol^{-1})
MagLS	20	6.26	4.17×10^{-4}	0.882	1.19×10^{-4} (103.88 mg/g)	10.62×10^4	1.25×10^{-8}	0.986	2.05×10^{-4}	1.42×10^{-9}	0.924	18.74
	30	5.07	6.23×10^{-4}	0.899	1.26×10^{-4} (109.99 mg/g)	17.82×10^4	7.47×10^{-9}	0.994	2.46×10^{-4}	1.63×10^{-9}	0.939	17.49
	40	5.27	6.08×10^{-4}	0.909	1.32×10^{-4} (115.23 mg/g)	19.83×10^4	6.71×10^{-9}	0.996	2.45×10^{-4}	1.55×10^{-9}	0.938	17.97
LS	20	4.30	6.46×10^{-4}	0.858	1.11×10^{-4} (96.89 mg/g)	40.39×10^4	3.29×10^{-8}	0.991	2.32×10^{-4}	2.09×10^{-9}	0.894	15.47

(115.23 mg/g) for LS and MagLS, respectively. q_{max} values also indicated that the surface modification produced improvement in the sorption capacity of LS towards dye molecules. The sorption capacity of the modified biomaterial exhibited an increasing trend with temperature rising as mentioned previously. Furthermore, all R_L values fall between 0 and 1 in Table 2 indicated the favorable sorption of RY2 molecules onto LS and Mag LS at all studied temperatures.

3.5. Thermodynamics of the sorption process

RY2 sorption of MagLS was monitored at three different temperatures (20, 30 and 40 °C) under the preoptimized conditions. The thermodynamic parameters (the values of change of free energy, enthalpy and entropy) were calculated from the following equations:

$$\Delta G^o = -RT \ln K_L \quad (17)$$

$$\ln K_L = -\frac{\Delta G^o}{RT} = -\frac{\Delta H^o}{RT} + \frac{\Delta S^o}{R} \quad (18)$$

Table 3
Thermodynamic parameters for the biosorption of RY2 onto MagLS.

t (°C)	ΔG^o (kJ mol^{-1})	ΔH^o (kJ mol^{-1})	ΔS^o (kJ/K mol^{-1})
20	−28.18		
30	−30.46	23.43	0.18
40	−31.72		

where R is the constant (8.314 J/mol/K) and T is the absolute solution temperature in Kelvin. A plot of ln K_L as a function of $1/T$ (figure not shown) yields a straight line from which $\Delta H°$ and $\Delta S°$ were calculated from the slope and intercept, respectively. The values of these parameters are listed in Table 3. The negative $\Delta G°$ values (– 28.18 kJ/mol at 20 °C, – 30.46 kJ/mol at 30 °C and – 31.72 kJ/mol at 40 °C) indicated that the sorption of RY2 on MagLS is a spontaneous process. The decrease of $\Delta G°$ values with increasing temperature indicates that the sorption of RY2 on MagLS is more favorable at higher temperature. The positive value of $\Delta H°$ (23.43 kJ/mol) affirmed the endothermic nature of the

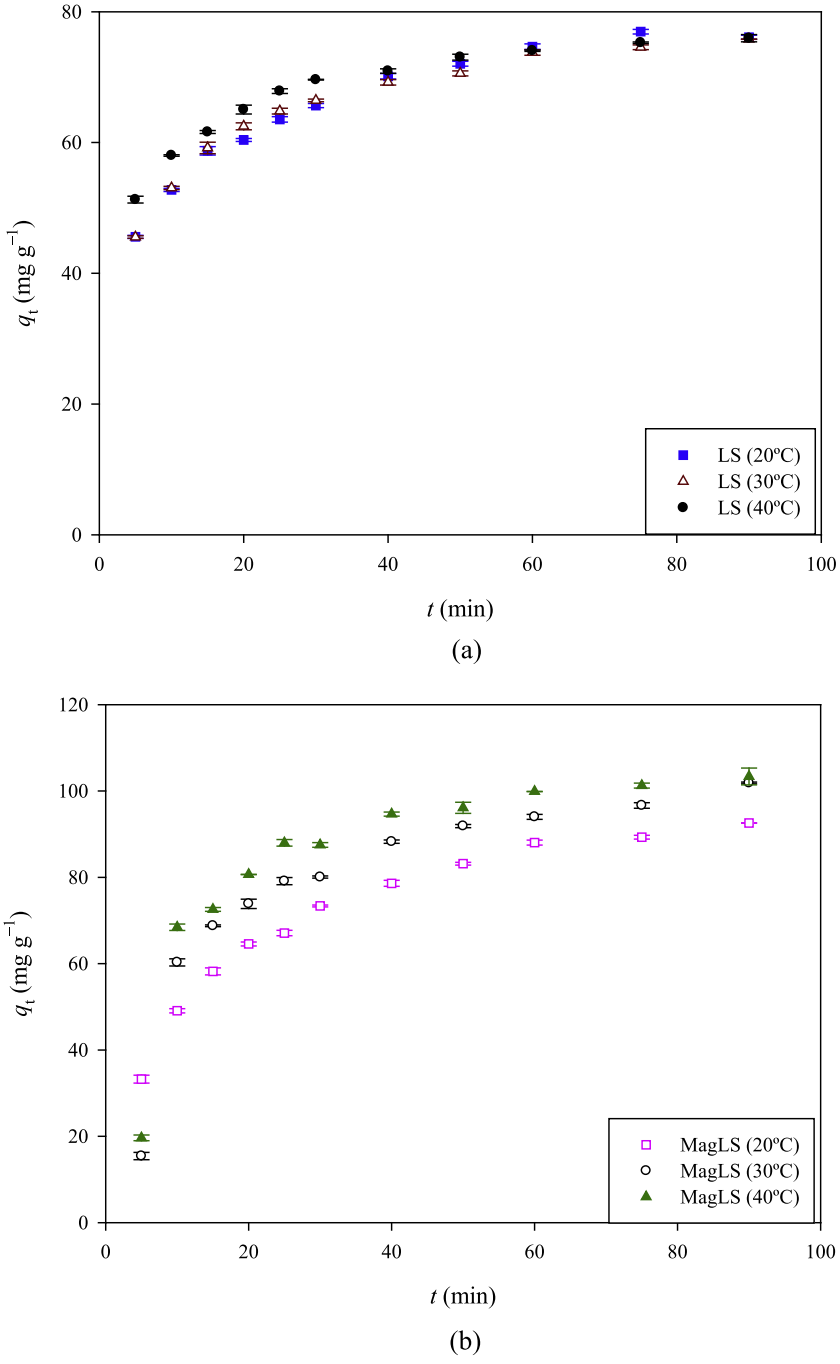

Fig. 4. Time profile of RY2 biosorption onto LS (a) and MagLS (b) at different temperatures.

process. Moreover, a positive value of ΔS^o indicated that randomness at the solid – solute interface increased with RY2 sorption onto the MagLS surface, suggested good affinity of dye molecules toward the sorbent and reflected some structural changes in sorbate and sorbent.

3.6. Continuous flow mode sorption

Continuous flow mode sorption potential is an important feature for suggested sorbent materials to evaluate their technical feasibility in wastewater tretament applications. To identify the dye sorption ability of MagLS in continuous mode, decolorization experiments were conducted with different flow rates and sorbent amounts. The results given in Fig. 6 indicated that lower flow rates resulted in good sorption performances and therefore, dye solutions were passed through the columns at a flow rate of 1.0 mL/min. The sorption yields of the suggested material are decreased with the increasing flow rate. The reason for this behavior is the lower contact time between dye molecules and sorbent surfaces at higher flow rates. A similar tendency has been reported for Congo Red removal process using jujuba shell [36].

The decolorization yields at different amount of MagLS packed into the columns were also shown in Fig. 7. The results indicated that the dye removal yield of the column increased from 13.68 to 59.24% by increasing MagLS amount in the column from 0.01 to 0.1 g. An increase of MagLS dosage could provide more specific surface of the sorbent material, which supplies more binding sites for dye molecules. No significantly change was observed in the

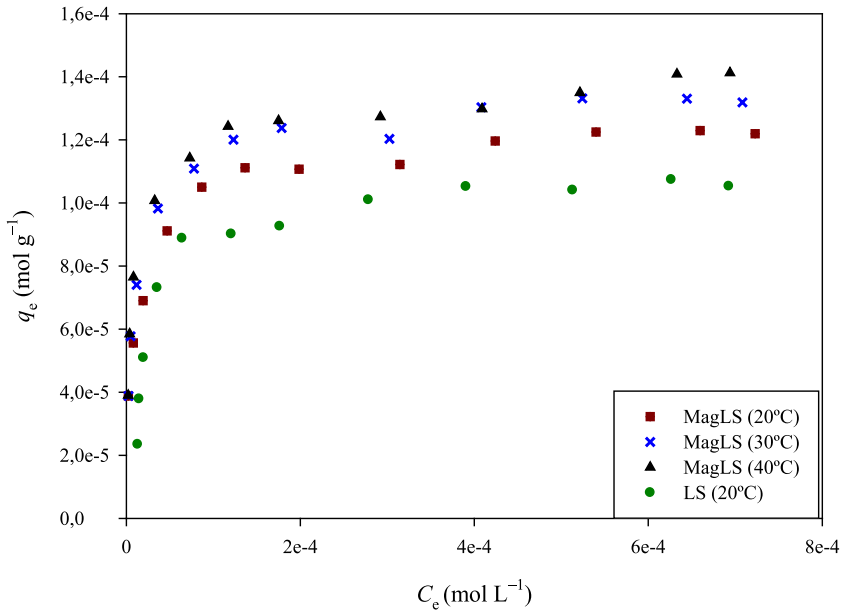

Fig. 5. General isotherm plots for RY2 biosorption onto MagLS and LS.

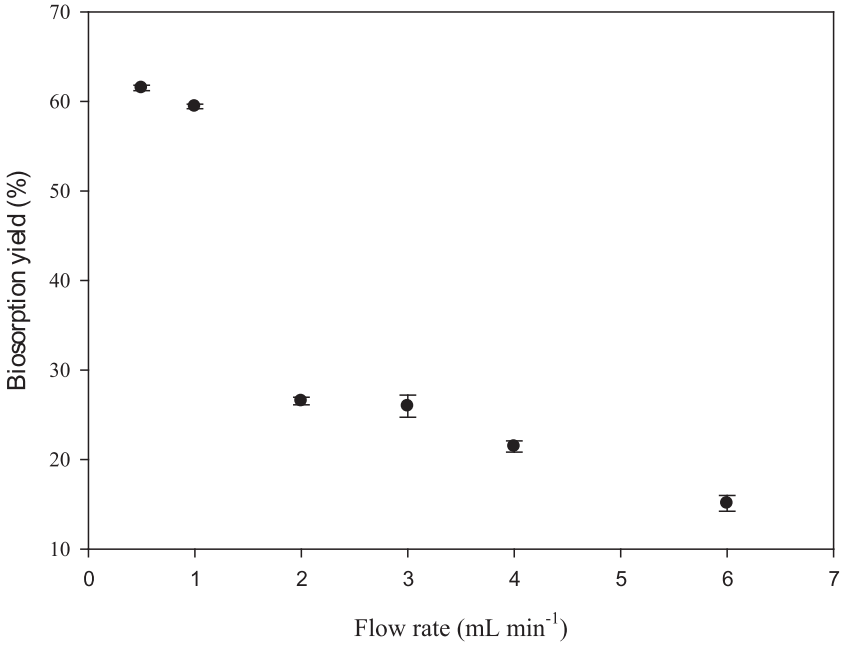

Fig. 6. Effect of flow rate on the biosorption of RY2 onto MagLS in continuous system.

decolorization yield above this point ($p > 0.05$) as a result of the saturation of dye binding sites on the sorbent surface. This finding was similar to results obtained from sorbent amount optimization experiments in batch mode.

Dye removal performance of MagLS was also tested in real wastewater conditions for continuous flow and batch modes. Industial wastewater was obtained from casting unit of metal processing industry in Eskişehir, Turkey. It was spiked with 100 mg/L RY2. The wastewater includes cadmium (0.71 mg/L), manganese (0.21 mg/L), potassium (10.00 mg/L), calcium (187.30 mg/L) and magnesium (35.44 mg/L). The continuous flow and batch mode sorption yields of RY2 onto MagLS in this industrial wastewater was recorded as 73.03 and 81.40%, respectively. These good sorption performances can be considered an important advantage for the usability of MagLS in real wastewater conditions.

3.7. Breakthrough study

The pollutant removal performance of the packed bed columns is generally evaluated by the breakthrough curves. A breakthrough curve obtained for RY2 sorption onto MagLS at a constant flow rate of 1 mL/min, influent (RY2) concentration of 100 mg/L and sorbent amount of 0.5 g is shown in Fig. 8. The dye concentration in the effluent was too low and the breakthrough point emerged around 410 min. Dye concentration in the effluent gradually increased with interaction time ($p < 0.05$) and MagLS packed column reached to an exhausted point around 1220 min. These results demonstrated that MagLS could be effectively employed for a relatively long period in dynamic flow treatment process for RY2 contaminated solutions.

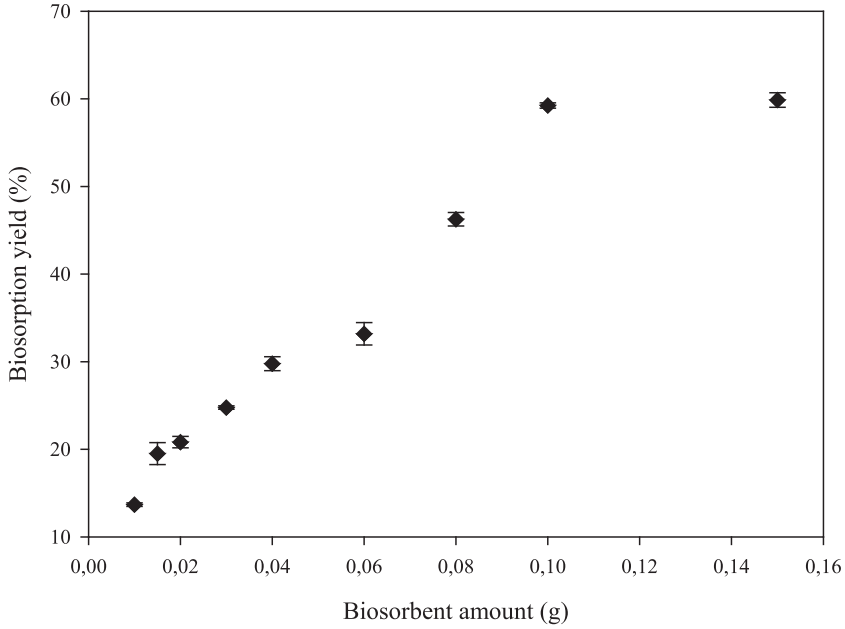

Fig. 7. Effect of biosorbent amount on the biosorption of RY2 onto MagLS in continuous system.

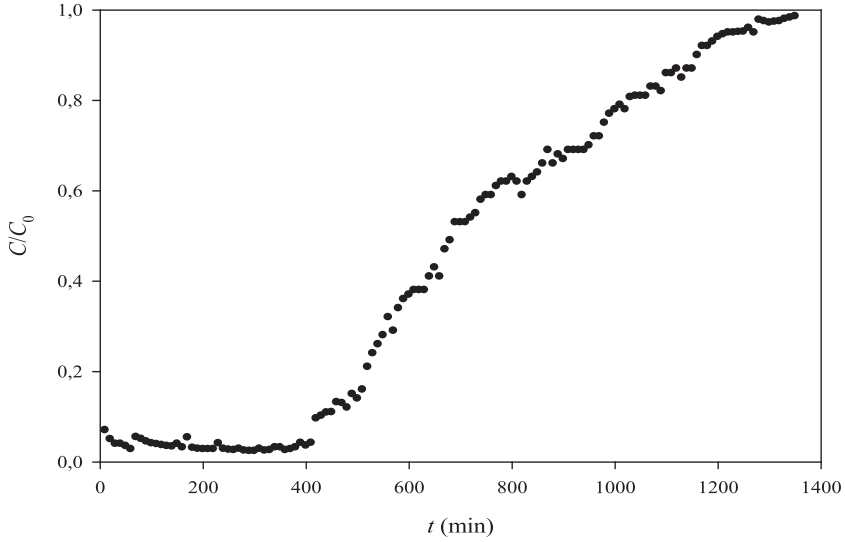

Fig. 8. Breakthrough curve for the biosorption of RY2 onto MagLS.

3.8. Regeneration and reusability of MagLS

Regeneration ability of a sorbent material is crucial factor for the economic feasibility of large scale treatment applications. Therefore, regeneration experiments were conducted to evaluate the reusability potential of MagLS in packed column. 0.01 M NaOH was used in these experiments as an eluent. Fig. 9 presents the performance of MagLS packed column during 25 consecutive cycles for RY2 sorption and desorption. The results obtained from regeneration studies indicated that MagLS possessed potential recycle performance especially upto 15 recycles with the high sorption and recovery yields. On the other hand a slight increase in the sorption yield of MagLS during these cycles may be explained by the activation effect of eluent similar to the chemical pretreatment. At the end of 25th cycle, around 80% recovery yield was still maintained. These results indicated that MagLS is a reusable sorbent material for convenient and efficient removal of RY2 from contaminated aquatic media.

3.9. Characterization

VSM measurements were performed at room temperature in order to determine the magnetic properties of the prepared sorbent material. The typical magnetization curve of MagLS is given in Fig. 10(a). The magnetic saturation value of MagLS was estimated to be 12.5 emu/g. Such magnetization value confirmed the magnetically modification of biomass. This feature makes MagLS very sensitive to external magnetic field and provides improved separation potential in the sorption applications.

Moreover, XRD patterns of LS and MagLS illustrated in Fig. 10(b) indicated that LS has amorphous structure. Dye molecules could easily penetrate through the LS surface. The XRD pattern of MagLS revealed the six characteristic peaks of Fe_3O_4 at about 30° (2 2 0), 35 ° (3 1 1), 43 ° (4 0 0), 53 ° (4 2 2), 57 ° (5 1 1) and 63 ° (4 4 0). It further confirms that the nano-Fe_3O_4 phase has been introduced into biomass surface, which made biomass magnetism.

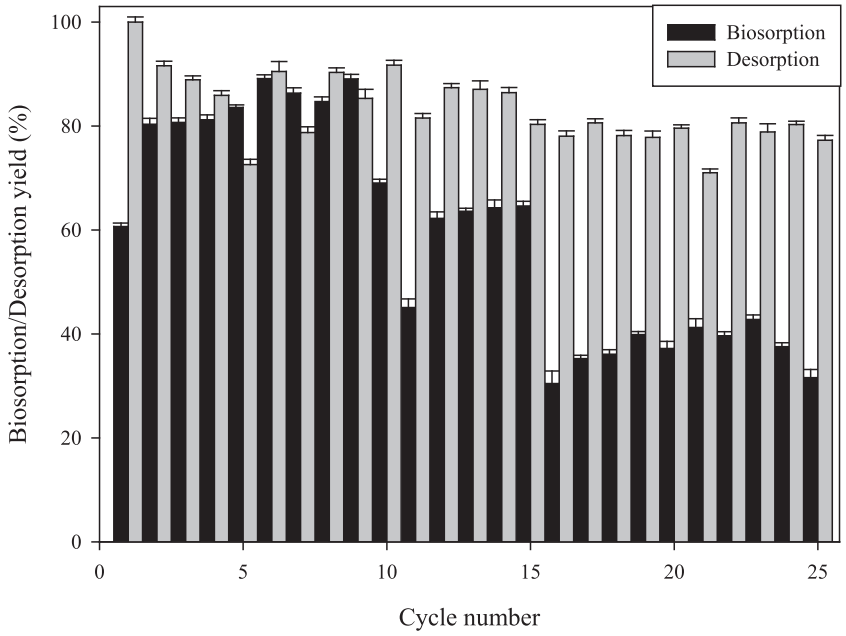

Fig. 9. Regeneration potential of MagLS in the RY2 biosorption.

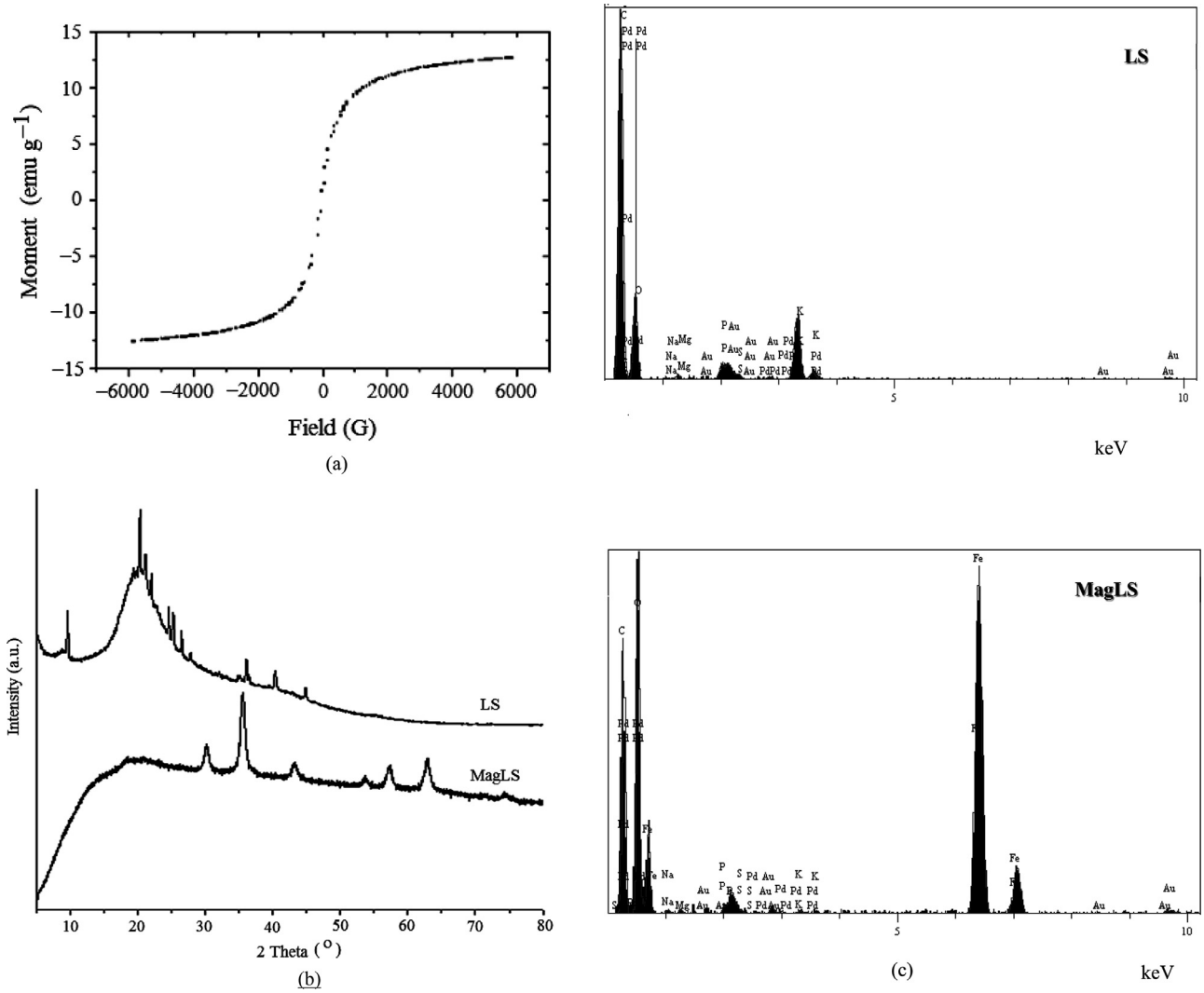

Fig. 10. VSM curve of MagLS (a), X-ray diffraction (XRD) patterns of LS and MagLS (b),EDX spectrum of LS and MagLS (c), SEM micrographs of LS, MagLS and dye loaded MagLS (d), IR spectra of MagLS and dye loaded MagLS (e).

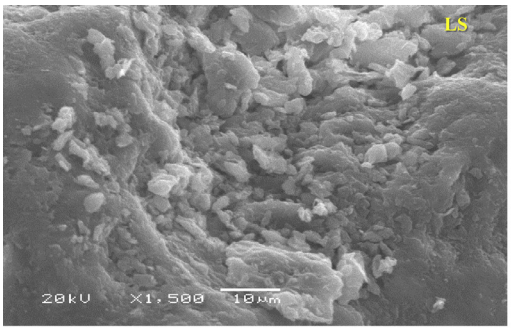

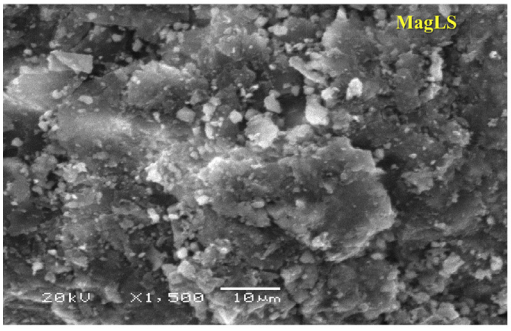

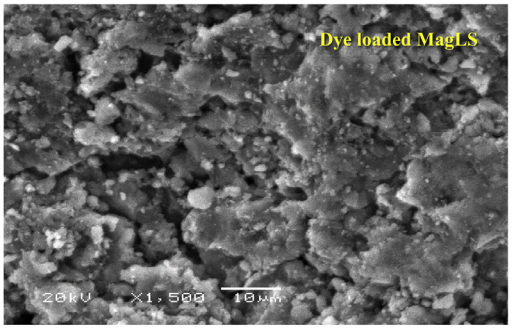

(d)

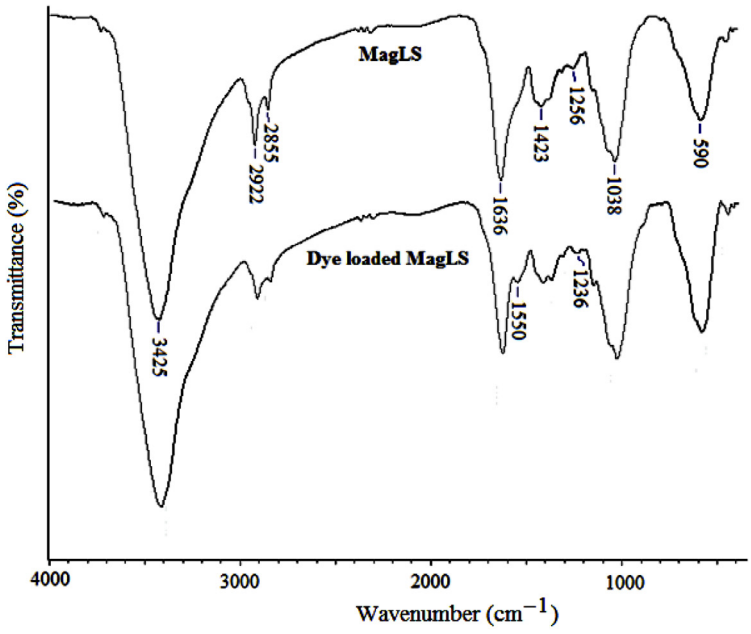

(e)

Fig. 10. Continued

Magnetic property of the sorbent material was also confirmed by the presence of prominent Fe peak in the EDX spectrum of MagLS, which is absent in the EDX spectrum of LS (Fig. 10(c)). On the other hand, SEM micrographs of LS, MagLS and RY2 loaded MagLS are given in Fig. 10(d). It can be seen from the figure that, the heterogenous and granular surface structure of LS becomes more smooth and rough after the magnetic modification. Also there is a great number of new agglomerations and shiny particles attracts attention in the micrograph of dye loaded MagLS. This finding could be attributed to coverage of MagLS surface by dye molecules.

IR spectra of rigid MagLS and RY2 – loaded MagLS are presented in Fig. 10(e). IR spectrum of MagLS shows a band located around 3425 cm^{-1}, which is attributed to –OH and –NH stretching vibrations. Symetric and asymmetric stretchings of $-CH_3$ and $-CH_2$ groups were seen at 2922 and 2855 cm^{-1}. The strong absorption bands observed at 1636 and 1038 cm^{-1} which are attributed to C = O and P–OH strecthing vibrations, respectively. Moreover, a band at 1256 cm^{-1} can be ascribed to C – O group of MagLS [37]. The stretching band observed at 590 cm^{-1} is typically due to the characteristic peak of Fe – O of Fe_3O_4 and proves the magnetic character of the biomass. The infrared spectrum of RY2 loaded – MagLS shows the appearance of new peak at about 1550 cm^{-1} caused by –N = N– group of dye. The IR spectra of MagLS exposed to dye anions indicated no significant shifts or change in any of the characteristic absorbance bands present on the magnetic biosorbent with the exception of a band shift from 1256 to 1236 cm^{-1}. These results implied not only involvement of C – O in the sorption of dye, but also the possibility that dye removal could be taken place through electrostatic interaction, rather than complexation.

4. Conclusion

Our study showed that the magnetic biosorbent prepared from *L. salmonicolor* biomass had a significant potential for reactive dye removal from contaminate solutions due to its high sorption performance and low-cost. The sorption characteristics of RY2 dye onto MagLS were investigated by both the batch and dynamic flow mode treatments. The effective parameters including pH, initial dye concentration, sorbent amount and contact time were optimized by RSM. Maximum RY2 removal capacity of MagLS was 115.23 mg/g under optimized conditions. Higher determination of coefficient showed better agreement between experimental and predicted values. The decolorization process conformed to the Langmuir isotherm model. The pseudo – second – order kinetic model exhibited better fit to the sorption data of RY2 than the pseudo – first – order kinetic model. Intraparticle diffusion model fitted the decolorization data within the equilibrium time. MagLS packed columns provide high efficiency in dynamic flow mode

treatment. A positive entrophy value indicated increased randomness at the solid–solution interface after decolorization process. A positive enthalpy value showed that the process was endothermic in nature. Regeneration studies suggested that MagLS could be successfully reused up to 25 cycles. Overall, by taking into account of all the findings it can be concluded that MagLS can be considered as an alternative and effective sorbent material for the treatment of reactive dye contamination.

Acknowledgments

This study has been supported by the Commission of Scientific Research Projects of Eskişehir Osmangazi University (Project Number 201419A108).

Supplementary materials

Supplementary material associated with this article can be found, in the online version, at doi:10.1016/j.jtice.2018.09.001.

References

[1] Yao L, Zhang L, Wang R, Chou S, Dong Z. A new integrated approach for dye removal from wastewater by polyoxometalates functionalized membranes. J Hazard Mater 2016;301:462–70.
[2] Ahmad A, Mohd-Setapar SH, Chuong CS, Khatoon A, Wani WA, Kumar R, Rafatullah M. Recent advances in new generation dye removal technologies: novel search for approaches to reprocess wastewater. RSC Adv 2015;5(39):30801–18.
[3] Gadd GM. Biosorption: critical review of scientific rationale, environmental importance and significance for pollution treatment. J Chem Technol Biotechnol 2009;84(1):13–28.
[4] Vijayaraghavan K, Yun Y-S. Bacterial biosorbents and biosorption. Biotechnol Adv 2008;26(3):266–91.
[5] Park D, Yun YS, Park JM. The past, present, and future trends of biosorption. Biotechnol Bioproc E 2010;15(1):86–102.
[6] S-Y Wang, Y-K Tang, Li K, Mo Y-Y, Li H-F, Gu Z-Q. Combined performance of biochar sorption and magnetic separation processes for treatment of chromium-contained electroplating wastewater. Bioresour Technol 2014;174:67–73.
[7] He X, Che R, Wang Y, Li Y, Wan L, Xiang X. Core–nanoshell magnetic composite material for adsorption of Pb(II) in wastewater. J Environ Chem Eng 2015;3(3):1720–4.
[8] Šafaříková M, Ptáčková L, Kibriková I, Šafařík I. Biosorption of water-soluble dyes on magnetically modified Saccharomyces cerevisiae subsp.uvarum cells. Chemosphere 2005;59(6):831–5.
[9] Bai J, Wu X, Fan F, Tian W, Yin X, Zhao L, Fan F, Li Z, Tian L, Qin Z, Guo J. Biosorption of uranium by magnetically modified *Rhodotorula glutinis*. Enzyme Microb Technol 2012;51(6–7):382–7.
[10] Li H, Li Z, Liu T, Xiao X, Peng Z, Deng L. A novel technology for biosorption and recovery hexavalent chromium in wastewater by bio-functional magnetic beads. Biores Technol 2008;99(14):6271–9.
[11] Alencar WS, Acayanka E, Lima EC, Royer B, de Souza FE, Lameira J, Alves CN. Application of mangifera indica (mango) seeds as a biosorbent for removal of victazol orange 3R dye from aqueous solution and study of the biosorption mechanism. Chem Eng J 2012;209(0):577–88.
[12] Khadami R, Alizadeh A, Saeb K. Synthesis and application of modified magnetic nanoparticles for removal of Cyanide from aqueous solutions. Int J Nano Dimens 2014;5(3):241–6.
[13] Dong S, Wang Y. Characterization and adsorption properties of a lanthanum-loaded magnetic cationic hydrogel composite for fluoride removal. Water Res 2016;88:852–60.
[14] Song Y, Duan Y, Zhou L. Multi-carboxylic magnetic gel from hyperbranched polyglycerol formed by thiol-ene photopolymerization for efficient and selective adsorption of methylene blue and methyl violet dyes. J Colloid Interface Sci 2018;529:139–49.
[15] Cheng Z, Liao J, He B, Zhang F, Zhang F, Huang X, Zhou L. One-step fabrication of graphene oxide enhanced magnetic composite gel for highly efficient dye adsorption and catalysis. ACS Sustain Chem Eng 2015;3(7):1677–85.
[16] Li C, Wang X, Meng D, Zhou L. Facile synthesis of low-cost magnetic biosorbent from peach gum polysaccharide for selective and efficient removal of cationic dyes. Int J Biol Macromol 2018;107:1871–8.
[17] Safarik I, Rego LFT, Borovska M, Mosiniewicz-Szablewska E, Weyda F, Safarikova M. New magnetically responsive yeast-based biosorbent for the efficient removal of water-soluble dyes. Enzyme Microb Technol 2007;40(6):1551–6.
[18] Safarikova M, Pona BMR, Mosiniewicz-Szablewska E, Weyda F, Safarik I. Dye adsorption on magnetically modified *Chlorella vulgaris* cells. Fresen Environ Bull 2008;17:486–92.
[19] Zhang Q, Lu T, Bai D-M, Lin D-Q, Yao S-J. Self-immobilization of a magnetic biosorbent and magnetic induction heated dye adsorption processes. Chem Eng J 2016;284:972–8.
[20] Panneerselvam P, Morad N, Tan KA. Magnetic nanoparticle (Fe_3O_4) impregnated onto tea waste for the removal of nickel(II) from aqueous solution. J Hazard Mater 2011;186(1):160–8.
[21] Aslan N, Cebeci Y. Application of Box–Behnken design and response surface methodology for modeling of some Turkish coals. Fuel 2007;86(1–2):90–7.
[22] Pouralinazar F, Yunus MAC, Zahedi G. Pressurized liquid extraction of orthosiphon stamineus oil: experimental and modeling studies. J Supercrit Fluid 2012;62(0):88–95.
[23] Yetilmezsoy K, Demirel S, Vanderbei RJ. Response surface modeling of Pb(II) removal from aqueous solution by Pistacia vera L.: Box–Behnken experimental design. J Hazard Mater 2009;171(1–3):551–62.
[24] Lagergren S. Zur theorie der sogenannten adsorption gelöster stoffe. Kungliga Svenska Vetenskapsakademiens. Handlingar 1989;24:1–39.
[25] Ho YS, McKay G. Pseudo-second order model for sorption processes. Process Biochem 1999;34(5):451–65.
[26] Weber W J Jr, Morriss JC. Kinetics of adsorption on carbon from solution. J Sanit Eng Div Am Soc Civ Eng 1963;89:31–9.
[27] Langmuir I. The adsorption of gases on plane surfaces of glass, mica and platinum. J Am Chem Soc 1918;40:1361–403.
[28] Freundlich H. Über die absorption in lösungen. Z Phys Chem (Leipzig) 1906;57A:385–470.
[29] Dubinin M, Radushkevich L. Equation of the characteristic curve of activated charcoal. Chem Zentr 1947;1:875–90.
[30] Hall KR, Eagleton LC, Acrivos A, Vermeulen T. Pore- and solid-diffusion kinetics in fixed-bed adsorption under constant pattern conditions. Ind Eng Chem Fundam 1966;5:212–23.
[31] Hobson JP. Physical adsorption isotherms extending from ultrahigh vacuum pressure. J Phys Chem 1969;73:2720–7.
[32] Dalvand A, Nabizadeh R, Reza Ganjali M, Khoobi M, Nazmara S, Hossein Mahvi A. Modeling of reactive blue 19 azo dye removal from colored textile wastewater using L-arginine-functionalized Fe3O4 nanoparticles: optimization, reusability, kinetic and equilibrium studies. J Magn Magn Mater 2016;404:179–89.
[33] Karimifard S, Alavi Moghaddam MR. Enhancing the adsorption performance of carbon nanotubes with a multistep functionalization method: optimization of reactive blue 19 removal through response surface methodology. Process Environ Prot 2016;99:20–9.
[34] Inyinbor AA, Adekola FA, Olatunji GA. Kinetics, isotherms and thermodynamic modeling of liquid phase adsorption of rhodamine B dye onto *Raphia hookerie* fruit epicarp. Water Resour India 2016;15:14–27.
[35] Afroze S, Sen TK, Ang HM. Adsorption removal of zinc (II) from aqueous phase by raw and base modified Eucalyptus sheathiana bark: kinetics, mechanism and equilibrium study. Process Saf Environ Prot 2016;102:336–52.
[36] El Messaoudi N, El Khomri M, Dbik A, Bentahar S, Lacherai A, Bakiz B. Biosorption of Congo red in a fixed-bed column from aqueous solution using jujube shell: experimental and mathematical modeling. J Environ Chem Eng 2016;4(4, Part A):3848–55.
[37] Akar T, Celik S, Gorgulu Ari A, Tunali Akar S. Nickel removal characteristics of an immobilized macro fungus: equilibrium, kinetic and mechanism analysis of the biosorption. J Chem Technol Biotechnol 2013;88(4):680–9.